CrossMark

Drought trends based on the VCI and its correlation with climate factors in the agricultural areas of China from 1982 to 2010

Xiaojin Qian · Liang Liang ⦿ · Qiu Shen · Qin Sun · Lianpeng Zhang · Zhixiao Liu · Shuhe Zhao · Zhihao Qin

Abstract Drought is a type of natural disaster that has the most significant impacts on agriculture. Regional drought monitoring based on remote sensing has become popular due to the development of remote sensing technology. In this study, vegetation condition index (VCI) data recorded from 1982 to 2010 in agricultural areas of China were obtained from advanced very high resolution radiometer (AVHRR) data, and the temporal and spatial variations in each drought were analyzed. The relationships between drought and climate factors were also analyzed. The results showed that from 1982 to 2010, the agricultural areas that experienced frequent and severe droughts were mainly concentrated in the northwestern areas and Huang-Huai Plain. Moreover, the VCI increased in the majority of agricultural areas, indicating that the drought frequency decreased over time, and the decreasing trend in the southern region was more notable than that in the northern region. A correlation analysis showed that temperature and wind velocity were the main factors that influenced drought in the agricultural areas of China. From a regional perspective, excluding precipitation, the climate factors had various effects on drought in different regions. However, the correlation between the VCI and precipitation was low, possibly due to the widespread use of artificial irrigation technology, which reduces the reliance of agricultural areas on precipitation.

Keywords Agricultural area · Drought · VCI · Climate factor · Correlation coefficient

---

X. Qian · L. Liang (✉) · Q. Shen · Q. Sun · L. Zhang
School of Geodesy and Geomatics, Jiangsu Normal University, Xuzhou, China
e-mail: liangliang198119@163.com

L. Liang · S. Zhao · Z. Qin
School of Geographic and Oceanographic Sciences, Nanjing University, Nanjing, China

X. Qian
Key Laboratory of Digital Earth Science, Institute of Remote Sensing and Digital Earth, Chinese Academy of Science, Beijing, China

Z. Liu
College of Biology and Environment Science, Jishou University, Jishou, China

Introduction

Drought is one of the most costly types of disasters and can affect natural habitats, ecosystems, agricultural systems, and urban water supplies (Jiao et al. 2016). Nearly half of the countries in the world have suffered from drought (Field et al. 2012; Bokal et al. 2014; Masud et al. 2015). Therefore, it is critical to monitor and issue warnings about droughts. Agricultural drought refers to a lack of moisture for crops due to external environmental factors. Droughts impact normal crop growth and can cause crop failure (Wilhite 2000). Agriculture is the foundation of China's economy, and climate change is projected to directly influence food security and

sustainable development. Moreover, agriculture is severely constrained by the climate and weather (Dai 2013). Therefore, studies regarding agriculture drought and its relationship with climate factors have become popular among governments and researchers worldwide.

Currently, the common methods of agriculture drought monitoring can be divided into site-based and remote sensing-based indices. Site-based indices include the standardized precipitation index (SPI), Palmer drought severity index (PDSI), and crop moisture index (CMI). Remote sensing-based indices are divided into bare surface indices (e.g., thermal inertia and microwave moisture inversion) and vegetation cover indices (Liu et al. 2016). Site-based indices can be established based on precipitation, temperature, evaporation, runoff, and other meteorological and hydrological data from observation stations. However, it is difficult to continuously and dynamically monitor a wide range of drought areas using this method due to the limited spatial density of observation stations (Wang et al. 2012a; Zhou et al. 2014; Guo and Wang 2015; Hao et al. 2015).

With the development of remote sensing technology, it is possible to access extensive, multi-scale, and multi-temporal integrated surface information in real time and monitor a wide range of drought conditions (Wang et al. 2012b; Zhao 2013). A series of drought monitoring indices based on remote sensing data have been proposed, including the normalized difference vegetation index (NDVI) (Rouse et al. 1974), the temperature vegetation drought index (TVDI) (Sandholt et al. 2002), and the vegetation condition index (VCI) (Kogan 1995). Scholars have conducted numerous studies of the temporal and spatial distributions of regional droughts that affect crops based on these drought indices. For example, Ozelkan et al. (2016) estimated drought, which was expressed by SPI in a rain-fed and irrigated agricultural area in the heart of the Southeast Anatolia, Turkey, using Landsat 8 Operational Land Imager (OLI) NDVI data. The results showed positive correlations between SPI and NDVI over rain-fed areas and negative correlations over irrigated agricultural areas, and the best correlations between spring SPI and summer NDVI reflected the critical influence of spring watering on crop growth and summer yield in the region. Liu et al. (2014a) monitored the drought conditions in Jilin, China, during the plant growth period

using the TVDI based on moderate-resolution imaging spectroradiometer (MODIS) data and indicated that a large portion of the study area was humid from May to September 2005, drought occurred in the western part of the study area in August, and the eastern part of the study area was humid in June. Additionally, the approach accurately predicted the agriculture drought conditions in the study area during the crop growth season in 2005. Dutta et al. (2015) attempted to identify the spatiotemporal extent of agricultural drought over Rajasthan using VCI and assessed the performance of VCI by comparing the estimates to meteorological drought indicators. They found that VCI was useful for monitoring the onset, duration, and spatiotemporal extent of agricultural drought. In addition, many scholars have performed annual analyses of regional drought in recent years. For example, Ma and Fu (2006) analyzed annual drought in northern China using the surface humidity index, the PDSI, and inverted soil moisture and revealed the temporal and spatial variations of drought in the region over the past 54 years. He et al. (2011) analyzed the temporal and spatial characteristics of the frequency of extreme drought on inter-annual and inter-decadal scales and during summer and winter monsoons based on daily data from 108 meteorological stations in southwestern China from 1960 to 2009. Liang et al. (2014) analyzed the annual drought trends in China using the TVDI, which was calculated using MODIS data from 2001 to 2010, and drew conclusions regarding its relationship to climate factors. These studies provide a framework for agricultural drought monitoring and annual analyses of drought. However, the relationships between drought and climate factors must be investigated further and better understood, especially in agricultural areas.

In the indices based on vegetation cover, NDVI can only reflect the climate, soil, and thermal impacts on vegetation in an isolated and qualitative manner. From a macroscopic perspective, it is difficult to establish a unified and quantitative standard for assessing the growth conditions of crops; thus, VCI was proposed by Kogan. It includes the real-time NDVI information and historical information regarding NDVI change. Moreover, this method can decrease or eliminate the impacts on NDVI associated with different geographical locations, ecological systems, soil conditions, etc., as well as reflect crop water shortages (Kogan 1995; Liu and Kogan 1996). Based on the surface vegetation

growth conditions identified by satellite monitoring, the VCI evaluates drought based on changes in vegetation conditions, and its precision has been validated in many studies and applications. Furthermore, it is easier to calculate the VCI than the TVDI or other indices because the VCI can be calculated using data from the near-infrared and red bands. In addition, the sensitivity of the VCI for monitoring drought is significantly higher than that of the NDVI (Sha et al. 2013); therefore, the VCI has been widely used in drought monitoring and analysis (Cai et al. 1995; Domenikiotis et al. 2004; Bajgiran et al. 2008; Guan et al. 2008; Quiring and Ganesh 2010). The advanced very high resolution radiometer (AVHRR) is attached to National Oceanic and Atmospheric Administration (NOAA) satellites. The AVHRR can dynamically monitor large areas of vegetation because its data are characterized by long temporal series, high temporal resolution, and moderate spatial resolution.

Therefore, this study calculated the VCI using NOAA/AVHRR data and performed annual analyses of the temporal and spatial distributions of drought in agricultural areas in China from 1982 to 2010. Moreover, the correlations between the VCI and annual mean precipitation, temperature, sunshine duration, wind velocity, and atmospheric pressure were examined to understand the climate factors that influence droughts in China. These correlations provide a scientific basis for mitigating the impacts of climate change on agricultural production. The flowchart of the study is shown in Fig. 1.

Materials and methods

General description of the study area

China is a vast territory that can be divided into three natural regions based on differences in geographical location and natural and human geography: the eastern monsoon region, the northwestern arid and semi-arid region, and the Qinghai-Tibet alpine region. The eastern monsoon region is divided into northern and southern regions that are bounded by the Qinling Mountains and Huaihe River (January 0 °C isothermal and 800 mm isohyet). Thus, China can be divided into the following four geographic areas: the southern region (103°–123° E, 22°–34° N), northern region (103°–135° E, 33°–53° N), northwestern region (73°–123° E, 37°–50° N), and Tibetan Plateau (73°–104° E, 27°–40° N) (Liang et al. 2014). To better analyze the agricultural areas, they are divided into four regions according to the boundaries of the four geographic areas in China because it is difficult to describe the boundaries of agricultural areas in detail.

The study evaluates the correlations between drought and climate factors; therefore, the climate conditions in these agricultural areas of China should be introduced briefly. The annual mean precipitation decreases from the southeast coast to the inland northwest. The annual mean precipitation is more than 1600 mm in southeast coast areas and less than 50 mm in the majority of northwest inland areas. The latitude range of agricultural areas is extensive, and the temperature varies accordingly. In winter, the lowest temperature is lower than
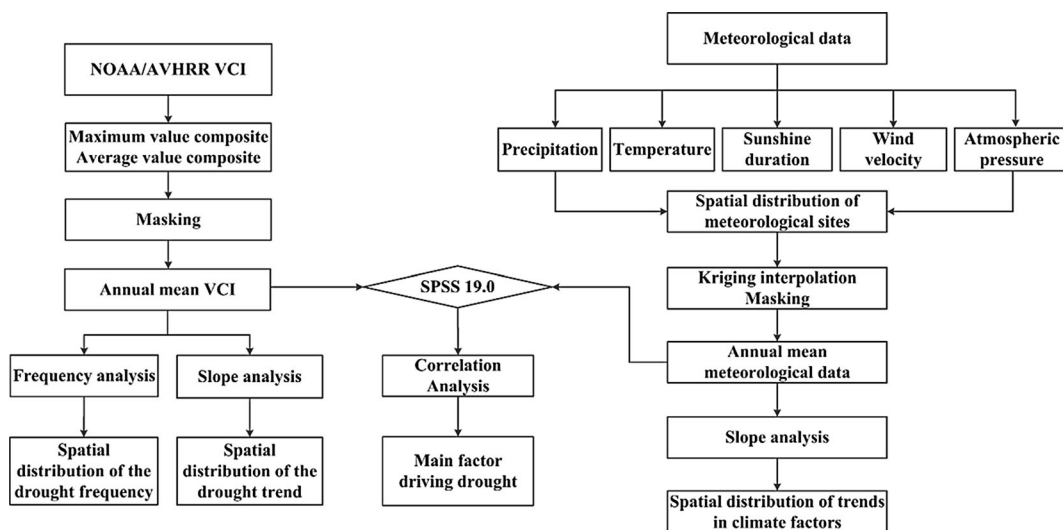

Fig. 1 Flowchart of the method

minus 30 °C, while the highest temperature is above 20 °C. The annual mean sunshine duration exhibits the opposite trend as that of the precipitation distribution. In the northwestern region and Tibetan Plateau, the annual mean sunshine duration is generally more than 3000 h, but in most southern region, it is less than 2000 h. The annual mean wind velocity is higher in northern and coastal areas than that in southern and inland areas. Notably, the annual mean wind velocity in coastal areas and three northern regions (northeast, northwest and northern China) is the largest in agricultural areas. China has a typical continental monsoon climate. In plain areas, winter is characterized by cold temperatures and high atmospheric pressure, while summer is characterized by high temperatures and low pressure. Therefore, the highest atmospheric pressure generally appears in January, and the lowest pressure occurs in July and August. However, the months with the highest and lowest atmospheric pressures are reversed in areas with elevations of 4000–5000 m compared (http://www.cma.gov.cn).

According to the second national land survey, there is approximately 135.385 million hectares of cultivated land, including paddy fields and dry land, in China, as shown in Fig. 2. The eastern region, which includes 26.297 million hectares of cultivated land, accounts for 19.4 % of the arable land in China, and the cultivated land primarily consists of paddy fields, which are generally used to plant rice, rapeseed, sugar cane, and other crops. The central area contains 30.715 million hectares of arable land, which accounts for 22.7 % of the arable land in China and is mainly used to grow wheat, rice, and cotton. The western cultivated land area covers 50.435 million hectares or 37.3 % of the arable land in China. This area is in an arid or extremely arid climate zone with an annual precipitation of less than 200 mm. However, the region has numerous inland rivers, which make it a commodity grain and cotton production base in China (Guan et al. 2008). The northeastern region, which contains 27.938 million hectares of cultivated land, accounts for 20.6 % of the arable land in China and is mainly dry land that is typically planted with wheat, beans, peanuts, and sugar beets (http://www.mlr.gov.cn/).
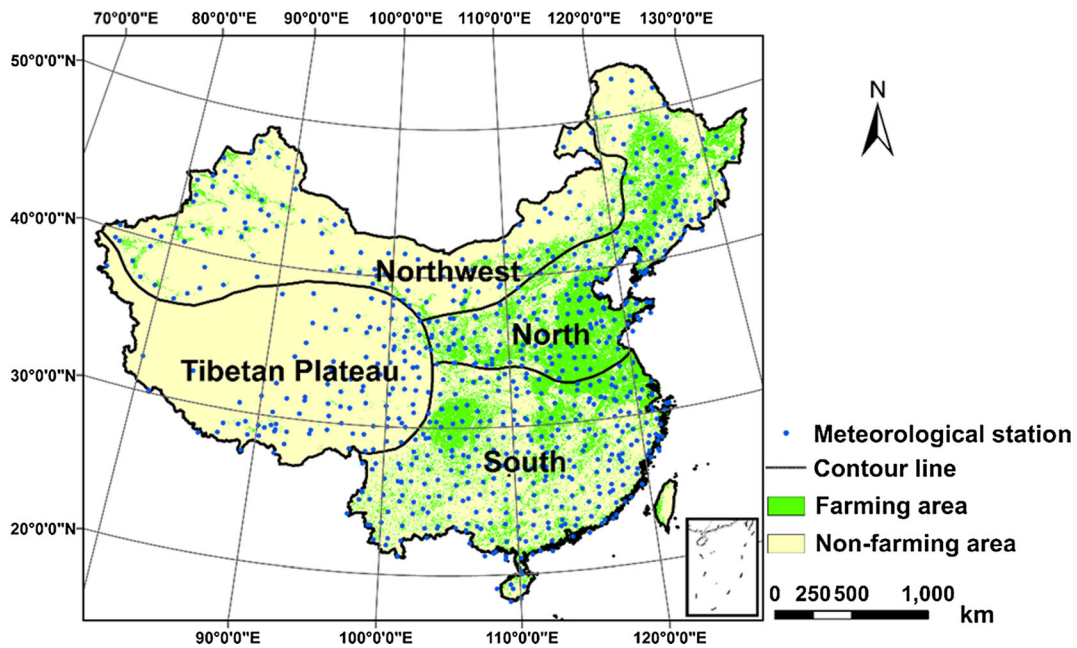
Acquisition of the VCI and meteorological data

The AVHRR data are provided by VHP vegetation health products from NOAA, which include three indexes: VCI, TCI, and VHI. The VCI, which spans 52 periods in a year, was obtained using IDL programming, and its spatial resolution is 16 km and temporal resolution is 7 days. Then, monthly data were synthesized using the maximum value composite method, and annual data were obtained using the average value composite method. The VCI was calculated using the following formula (Mao et al. 2005; Mao et al. 2007):

$$\text{VCI} = 100 \times \frac{\text{NDVI}_i - \text{NDVI}_{\min}}{\text{NDVI}_{\max} - \text{NDVI}_{\min}}$$

where NDVI_i is the NDVI of the pixels in a specific period, and $\text{NDVI}_{\max}$ and $\text{NDVI}_{\min}$ are the maximum and minimum NDVI values in a specific period, respectively. The maximum and minimum values of the denominator reflect the best and worst conditions for vegetation growth, respectively, and the difference between them reflects the living conditions of the local vegetation. The numerator is the difference between the known and minimum values of the NDVI for a specific period, which reflects the vegetation growth. A smaller value indicates that less vegetation grew. The VCI is calculated using this formula, which results in a number ranging from 0 to 100. If the VCI ranges from 70 to 100, it indicates normal vegetation conditions and no drought. A value between 50 and 70 indicates moderate vegetation conditions and mild drought, whereas a value from 30 to 50 indicates poor vegetation growth and moderate drought, and below 30 indicates extremely poor growth conditions and severe drought. Larger values of the VCI indicate good vegetation growth and low degrees of drought, whereas smaller values of the VCI indicate poor vegetation growth and higher degrees of drought (Sha et al. 2013; Dutta et al. 2015).

The National Meteorological Information Center in China provided 557 effective site observations of ground-recorded meteorological data from 1982 to 2010, as shown in Fig. 2. The monthly mean precipitation, air temperature, sunshine duration, wind velocity, and atmospheric pressure were calculated using the daily observation data from each site. The annual mean meteorological values were then determined based on the monthly mean values. Kriging interpolation was used to generate a raster map of the meteorological data with a spatial resolution of 1000 m. Then, the data in the agricultural areas were obtained by masking.

Fig. 2 Spatial distributions of agricultural areas and meteorological sites in 2010

Analysis of trends in the drought distribution and climate factors in agricultural areas from 1982 to 2010

To analyze changes in the trends of the VCI and the climate factors in agricultural areas from 1982 to 2010, the droughts were divided into four levels—normal (VCI $\geq$ 70), mild ($50 \leq$ VCI < 70), moderate ($30 <$ VCI < 50), and severe (VCI ≤ 30)—based on literature concerning aridity classification standards (Guan et al. 2008; Sha et al. 2013; Dutta et al. 2015). The corresponding grades of the VCI values are shown in Table 1. Then, different levels of drought frequency (f) were calculated using the following formula:

$$ f = \frac{n}{N} $$

where f is the drought frequency, n is the number of different levels of drought, and N is the length of the study

Table 1 Classification of the VCI

Level	VCI value
Normal	≥ 70
Mild drought	$50 \leq$ VCI < 70
Moderate drought	$30 <$ VCI < 50
Severe drought	≤ 30

period (27 years; there are no data from 1994 and 2000). In the following study, the total drought frequency and different levels of drought frequency will be analyzed. However, the total drought frequency is the sum of the mild drought, moderate drought, and severe drought frequencies. Therefore, in the total drought frequency analysis, a frequency up to 0.8 is considered a high frequency and 0.4 is considered a low frequency. However, in different levels of drought frequency analysis, a frequency of up to 0.6 is considered a high frequency and 0.2 is considered a low frequency.

In addition, the trends in the VCI and climate factors were calculated using the following formula to analyze the associated changes in agricultural areas (Zhang et al. 2011b):

$$ \text{Slope} = \frac{n \times \sum_{i=1}^{n} x_i t_i - \left(\sum_{i=1}^{n} x_i\right)\left(\sum_{i=1}^{n} t_i\right)}{n \times \sum_{i=1}^{n} t_i{}^2 - \left(\sum_{i=1}^{n} t_i\right)^2} $$

where x_i is the VCI or the value of a climate factor in year i, n is the length of the time series, and t_i is the number of the year from 1982 to 2010 (1–27). A positive slope indicates that the VCI or climate factor increased during the study period. Otherwise, the value decreased. The increasing trend in the VIC reflects improved vegetation growth and drought abatement. Thus, the VCI trend contrasts the drought trend. The

legends of the figures of drought and climate factor trends were mainly based on positive-negative properties or spatial distributions.

Correlation analysis of the VCI and climate factors

The Pearson correlation coefficient can reflect the degree and direction of the correlation between two variables. A larger absolute value indicates a stronger correlation between the two variables. The partial correlation coefficient is an indicator that measures the degree of linear correlation between two variables among several variables when the impacts of multiple other variables are controlled. The internal linear relationships between two variables can be more accurate and reliable by comparing the partial correlation coefficient and the correlation coefficient (Yan 2003). The Pearson correlation coefficients and partial correlation coefficients were calculated using SPSS 19.0 (IBM SPSS Inc., Chicago, USA) to analyze the relationships between drought and various climate factors. Correlation coefficients were calculated using the following formula:

$$R_{xy} = \frac{\sum_{i=1}^{n}\left(x_i - \overline{x}\right)\left(y_i - \overline{y}\right)}{\sqrt{\sum_{i=1}^{n}\left(x_i - \overline{x}\right)^2}\sqrt{\sum_{i=1}^{n}\left(y_i - \overline{y}\right)^2}}$$

where R_{xy} is the correlation coefficient, n is the length of the time series, and i is the number of the year from 1982 to 2010 (1–27). x_i and y_i are the VCI and the value of a climate factor in year i, respectively, and $\overline{x}$ and $\overline{y}$ are the mean VCI and the mean value of a climate factor, respectively, from 1982 to 2010.

Based on the linear correlation coefficient calculations, the partial correlation coefficient was calculated using the following formula:

$$R_{xyz} = \frac{R_{xy} - R_{xz}R_{yz}}{\sqrt{\left(1 - R_{yz}^2\right)\left(1 - R_{xz}^2\right)}}$$

"where R_{xyz} is the partial correlation coefficient of variables x and y after fixing variable z, R_{xy} is the correlation coefficient of variables x and y, R_{xz} is the correlation coefficient of variables x and z, and R_{yz} is the correlation coefficient of variables y and z.

Results and analysis

Analysis of the spatial and temporal distributions of drought in agricultural areas from 1982 to 2010

Analysis of the distribution of drought frequency

The spatial distribution of the drought frequency in agricultural areas of China was determined using NOAA/AVHRR data from 1982 to 2010. The results are shown in Fig. 3. The drought frequency in the vast majority of agricultural areas was greater than 0.6, and it

Fig. 3 Spatial distribution of the drought frequency
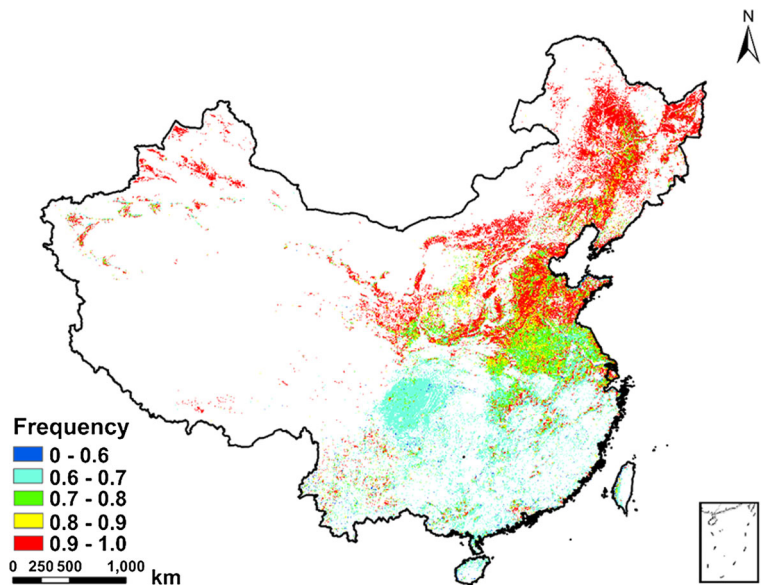
was greater than 0.8 in the northern and northwestern regions. Drought on the Northeastern Plain is caused by the excessive reclamation of cultivated land, which decreases the wetland area and reduces the ability of the soil to supply and store water, and by the destruction of the vegetation environment via the mining of mineral deposits, construction of reservoirs and dams, and overgrazing. In addition, less rain has led to serious desertification. Such high drought frequencies mainly occur because the Huang-Huai Plain is located in a humid and semi-humid climate zone; therefore, the temperature in this region increases rapidly before rain events occur, which causes substantial evaporation of soil moisture. Moreover, high population and industry densities in districts increase the demand for water and decrease surface runoff, which increases the drought

severity (Zhang et al. 2011a). However, severe drought in the northwest is largely caused by its specific geographical environment. This region is located inland, away from the ocean, and lacks precipitation; therefore, the drought frequency is comparatively high. The drought frequency in the southern agricultural areas was relatively low, but in some areas, such as Yunnan, it remained high, possibly due to the climate, the landform, and other natural factors, as well as poor cultivation practices, inadequate water conservancy strategies, and other human-induced factors (Yin and Li 2013). In general, the drought frequency was generally high in the northern agricultural areas and low in the southern areas. Additionally, the agricultural areas that experienced frequent droughts were mainly concentrated in the northern and northwestern areas.
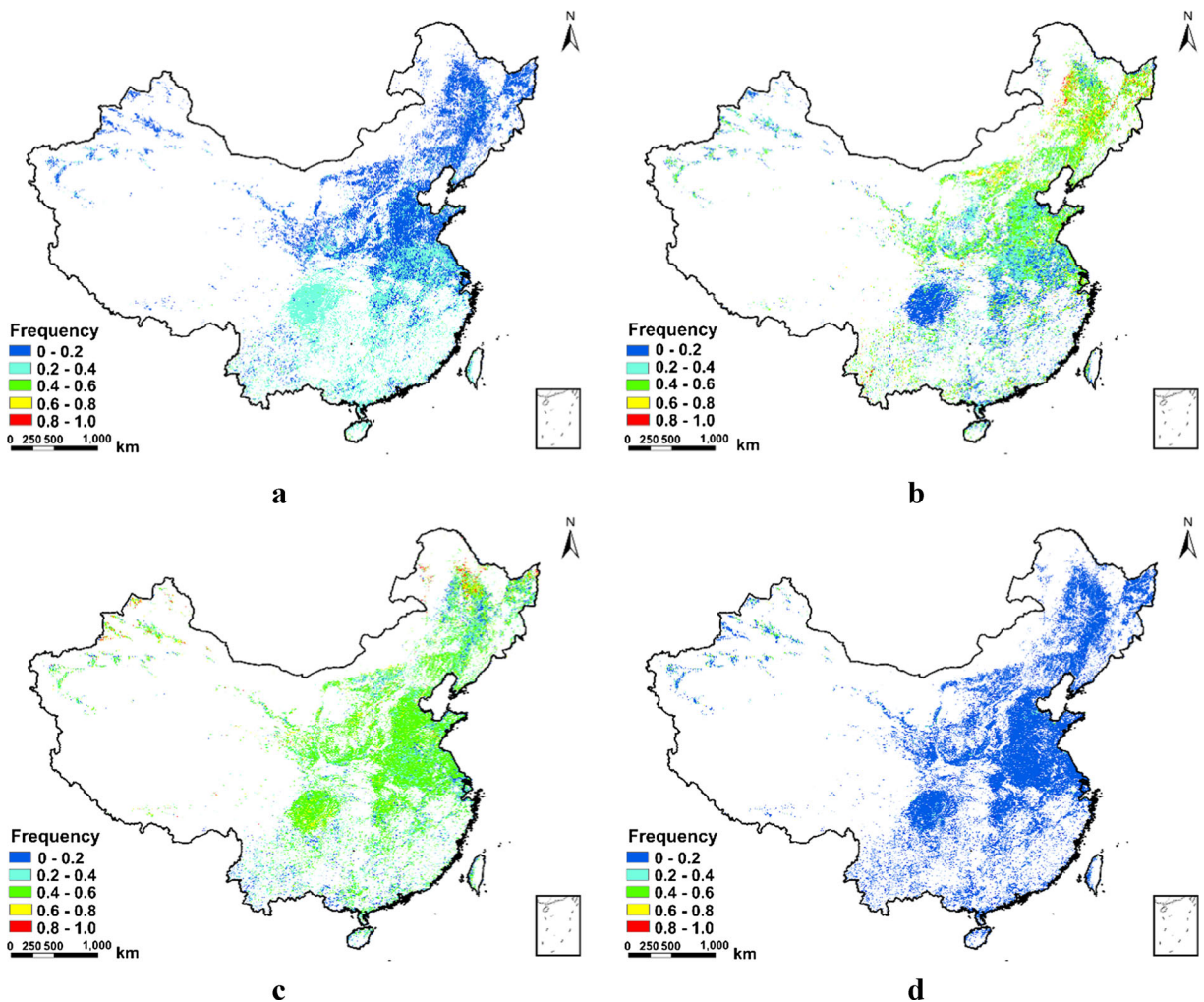

Fig. 4 Spatial distribution of drought frequency at different levels (**a** normal, **b** mild drought, **c** moderate drought, **d** severe drought)

Analysis of the distribution of the frequency of drought at different levels

As shown in Fig. 4, the frequency of drought at each of the four drought levels, normal, mild, moderate, and severe, was calculated. Then, the significant differences between the frequencies of drought at these levels were identified. The regions that had high normal frequencies were mainly concentrated in the southern regions, especially in the Sichuan Basin, which experienced no drought for approximately 40 % of the 27 years. The frequency in the northeastern and northwestern regions was zero, which indicates that drought persisted in these regions. The frequency of mild drought exhibited a certain variation with latitude and tended to decrease gradually from north to south. The mild drought frequency in most of the Northeastern Plain was at least 0.6, and the frequency in the Huang-Huai Plain and the southern region was lower than 0.4. In addition to the few extreme areas in the northeastern and northwestern regions, the frequency of moderate drought was concentrated in the 0.4 to 0.6 range. In most agricultural areas, the frequency of severe drought was zero. The frequency was low, i.e., less than 0.2, in the northwestern and central regions and on the Huang-Huai Plain. The analysis of the four levels of drought revealed a considerable difference in the drought frequency in the Sichuan Basin. The levels were typically normal and moderate, which were attributed to the unbalanced spatio-temporal distribution of precipitation because of the terrain, abnormal atmospheric circulation, regional climate variations, and other factors. In general, the majority of the national agricultural areas were affected by various degrees of drought. The Northeastern Plain mainly experienced mild droughts, whereas the Huang-Huai Plain and central region experienced moderate droughts, and the northwestern region experienced moderate and severe droughts. However, most agricultural areas were affected by mild and moderate droughts.

Analysis of the distribution of the drought trends

The spatial distribution of drought trends is shown in Fig. 5. Overall, the VCI increased in the vast majority of agricultural areas, especially in the Sichuan Basin, suggesting that the drought trend decreased over time. However, in a few agricultural areas, such as parts of the Middle-Lower Yangtze Plain, the Northeastern Plain, Ningxia, Gansu, northern Xinjiang, Mongolia, and so on, the VCI decreased, suggesting that the drought severity gradually increased from 1982 to 2010. In recent years, the urbanization process has accelerated, and wetland areas have been significantly reduced. These may be the dominant factors behind drought occurrence in the Yangtze River Delta.
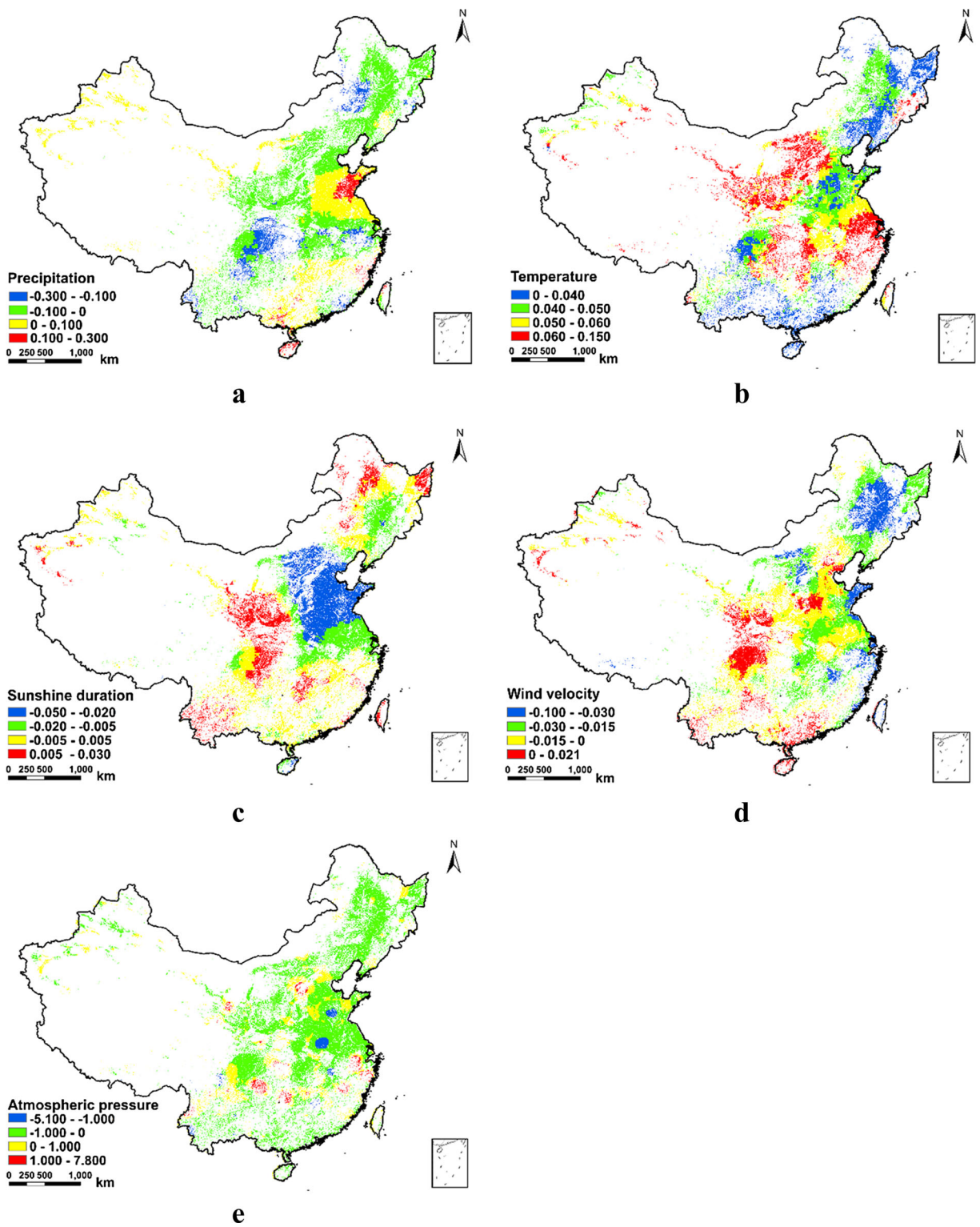
Climate factor trends in the agricultural areas of China from 1982 to 2010

The trends in the annual mean precipitation, temperature, sunshine duration, wind velocity, and atmospheric

Fig. 5 Spatial distribution of the drought trend
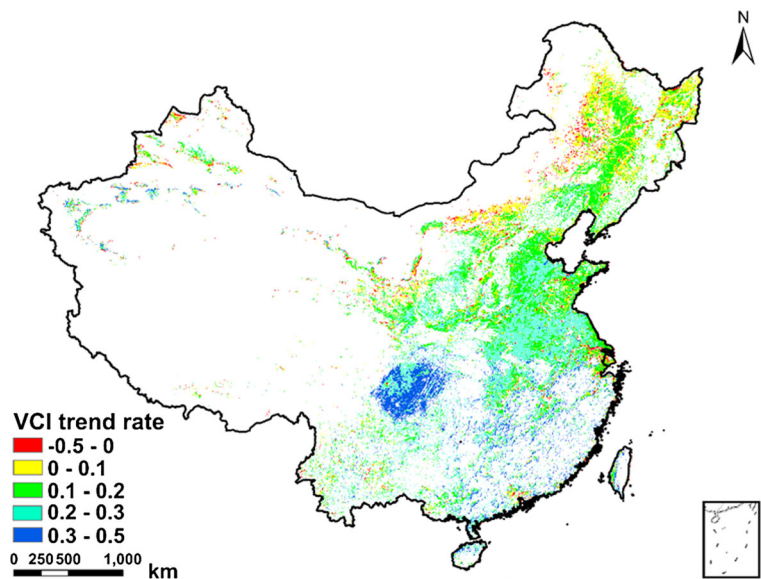
Fig. 6 Spatial distribution of trends in climate factors (**a** annual mean precipitation, **b** annual mean temperature, **c** annual mean sunshine duration, **d** annual wind velocity, **e** annual atmospheric pressure)

pressure are shown in Fig. 6. The mean precipitation exhibited a significant increasing trend in the Huang-Huai Plain area, especially in the central part of Shandong. This trend occurred because regional terrain lifting causes coastal water vapor to condense, which increases the amount of rain. In the Northeastern Plain, the Middle-Lower Yangtze Plain, and many areas in the central region, the mean precipitation exhibited a clear decreasing trend. In the agricultural areas of China, the mean temperature generally increased, which was consistent with the global warming phenomenon, especially in the Middle-Lower Yangtze Plain and Loess Plateau. However, the change was not apparent in the Northeastern Plain, the middle of the Huang-Huai Plain, the western Sichuan Basin, and parts of Guangxi and Yunnan. The overall trend in the mean sunshine duration was small. The trend decreased in the Huang-Huai Plain, the Middle-Lower Yangtze Plain, and the southern part of the Northeastern Plain, whereas the trend increased in mid-western China and the northern part of the Northeastern Plain. Regarding the mean wind velocity, an increasing trend was mainly concentrated in the Sichuan Basin and parts of Shan-Gan-Ning, and the trend decreased in the majority of the other regions, especially the eastern coastal areas, Shandong peninsula, and the middle of the Northeastern Plain. The regional differences in the mean atmospheric pressure were more significant. At the junction of Anhui, Henan, and mid-western Shandong, a decreasing trend was notable, whereas significant increasing trends appeared in Gansu, Shanxi, and several southern areas. The changes in other regions were small, but there was a decrease in the majority of these areas. In summary, the trends of the climate factors exhibited temporal and spatial differences from 1982 to 2010. The annual mean sunshine duration generally remained the same, and changes in

the precipitation and atmospheric pressure were relatively apparent. These changes may be related to changes in atmospheric circulation and ocean currents.

Analysis of the correlation between the VCI and the climate factors in the agricultural areas of China

To analyze the correlations between the VCI and climate factors, this study included calculations of the correlation coefficients between the VCI and the annual mean precipitation, temperature, sunshine duration, wind velocity, and atmospheric pressure, as shown in Table 2. The results showed that the VCI in agricultural areas had a significant positive correlation with the mean temperature, indicating that an increase in the mean temperature caused an upward trend in the VCI, which reflected a decline in drought. A statistical analysis showed that the maximum mean temperature was approximately 25 °C in southern agricultural areas, approximately 15 °C in the northern region, and approximately 11 and 12 °C in the northwestern region and Tibetan Plateau, respectively. These values did not exceed the most suitable temperature for growing the vast majority of crops (Liu et al. 2014b). In addition, this increase in temperature promoted vegetation growth to a certain extent, which led to higher values of the VCI. Conversely, the correlation between the VCI and the mean wind velocity was highly negative because a high wind velocity leads to greater evaporation and more rapid loss of surface moisture, which intensify drought conditions. The relationship between the VCI and mean sunshine duration was not significant in the agricultural areas of China, except for in the northern region. The VCI was slightly correlated with mean precipitation, partly because artificial irrigation has become popular in China, and a relatively complete water conservancy system that has been established

Table 2 Correlation coefficients of the VCI and climate factors in agricultural areas (time scale 1 year)

Region	Mean precipitation	Mean temperature	Mean sunshine duration	Mean wind velocity	Mean atmospheric pressure
Southern	−0.174	0.802**	0.028	−0.712**	−0.299
Northern	0.069	0.632**	−0.426*	−0.745**	−0.441*
Northwestern	0.059	0.650**	−0.198	−0.679**	−0.294
Tibetan Plateau	0.111	0.789**	0.171	−0.415*	−0.416*
Total	−0.052	0.766**	−0.228	−0.761**	−0.382*

*The correlation is significant at the 0.05 level (two-tailed test)

**The correlation is significant at the 0.01 level (two-tailed test)

Table 3 Partial correlation coefficients between the VCI and climate factors in agricultural areas (time scale 1 year)

Region	Mean precipitation	Mean temperature	Mean sunshine duration	Mean wind velocity	Mean atmospheric pressure
Southern	−0.185	0.578	0.052	−0.341	−0.331
Northern	0.044	0.505	−0.136	−0.478	−0.453
Northwestern	0.355	0.353	0.236	−0.560	−0.603
Tibetan Plateau	0.346	0.508	0.488	−0.220	−0.648
Total	0.103	0.442	0.139	−0.442	−0.382

in recent years. Therefore, most cultivated areas rely mainly on artificial irrigation, and their dependence on precipitation has decreased, as has the influence of precipitation on drought.

As shown in Table 3, to more accurately represent the relationship between the VCI and climate factors in agricultural areas, the partial correlation coefficients were calculated. Overall, temperature and wind velocity were the main factors that influenced drought in the agricultural areas of China. From a regional perspective, temperature was the main factor the influenced drought in the southern region. Temperature, wind velocity, and atmospheric pressure were the main driving factors in the northern region, and those in the northwestern region were wind velocity and atmospheric pressure, whereas those in the Tibetan Plateau region were temperature, sunshine duration, and atmospheric pressure. This analysis illustrates that the relationship between the climate factors is relatively complex in the agricultural areas of China. The VCI is affected by temperature, sunshine duration, wind velocity, atmospheric pressure, human activities, and other factors, and no single factor fundamentally determines the level of drought in agricultural areas.

Discussion and conclusion

This study presented an analysis of the main factors that influence drought and provided a scientific basis for mitigating the impacts of climate change on agricultural production by analyzing drought trends and the relationships between the VCI and the climate factors in the agricultural areas of China from 1982 to 2010. We arrived at the following conclusions:

1. The drought frequency was high in the northern agricultural areas and low in the southern areas from 1982 to 2010. Additionally, the agricultural areas that suffered from frequent, severe droughts were mainly concentrated in the northwestern area and the Huang-Huai Plain. However, most agricultural areas were influenced by mild and moderate droughts. Moreover, the VCI increased in the overwhelming majority of agricultural areas, illustrating that drought exhibited a decreasing tendency over time, and the decreasing trend in the southern region was larger than that in the northern region.

2. The analysis showed that the climate factor trends in the agricultural areas of China were inconsistent from 1982 to 2010. The annual mean temperatures in the four regions increased, and this phenomenon was consistent with global warming. However, different areas and regions exhibited different increases. The trends in the other four types of climate factors differed between the geographical regions, and the mean atmospheric pressure varied significantly.

3. The analysis of the correlations between the climate factors and the VCI showed that temperature and wind velocity were the main factors that influenced drought in the agricultural areas of China, and there were several geographical differences in the factors that affected drought. Excluding precipitation, the climate factors affected drought differently in different regions. In addition, the VCI was slightly correlated with mean precipitation, likely due to the popularization of artificial irrigation systems and relatively complete water conservancy. This conclusion is in agreement with that of Liang et al. (2014). Furthermore, the comparison between the correlations and the partial correlation analysis of the climate factors and VCI showed that the correlations between the climate factors are relatively complicated, and no single factor can radically determine the level of regional drought.

Remote sensing data and the choice of the vegetation index are critical factors in analyses of the characteristics of the temporal and spatial distributions of drought in agricultural areas over long periods. With the rapid development of remote sensing technology and increasingly precise drought monitoring and research, more comprehensive and detailed analyses of drought scenarios will be performed by combining remote sensing data from multiple sources and a variety of drought indices in the agricultural areas of China.

References

Bajgiran, P., Darvishsefat, A. A., Khalili, A., & Makhdoum, M. F. (2008). Using AVHRR-based vegetation indices for drought monitoring in the northwest of Iran. *Journal of Arid Environments, 72*(6), 1086–1096. doi:10.1016/j.jaridenv.2007.12.004.

Bokal, S., Grobicki, A., Kindler, J., & Thalmeinerova, D. (2014). From national to regional plans—the integrated drought management Programme of the global water Partnership for Central and Eastern Europe. *Weather and Climate Extremes, 3*, 37–46. doi:10.1016/j.wace.2014.03.006.

Cai, B., Lu, W. J., & Zheng, X. J. (1995). Using meteorological satellite's VCI to monitor soil state. *Remote Sensing for Land & Resource, 4*, 45–50.

Dai, A. (2013). Increasing drought under global warming in observations and models. *Nature Climate Change, 3*, 52–58.

Domenikiotis, C., Spiliotopoulos, M., Tsiros, E., & Dalezios, N. R. (2004). Early cotton yield assessment by the use of the NOAA/AVHRR derived vegetation condition index (VCI) in Greece. *International Journal of Remote Sensing, 25*(14), 2807–2819. doi:10.1080/01431160310001632729.

Dutta, D., Kundu, A., Patel, N. R., Saha, S. K., & Siddiqui, A. R. (2015). Assessment of agricultural drought in Rajasthan (India) using remote sensing derived vegetation condition index (VCI) and standardized precipitation index (SPI). *Egyptian Journal of Remote Sensing and Space Science, 18*(1), 53–63. doi:10.1016/j.ejrs.2015.03.006.

Field, C. B., Barros, V., Stocker, T. F., Qin, D., Dokken, D. J., Ebi, K. L., et al. (2012). *Managing the risks of extreme events and disasters to advance climate change adaptation. A special report of working groups I and II of the intergovernmental panel on climate change*. Cambridge: Cambridge University Press.

Guan, X. D., Guo, N., Huang, J. P., Ge, J. M., & Zhang, Z. H. (2008). Applicability analysis of VCI to monitoring northwest China drought. *Plateau Meteorology, 27*, 1046–1053.

Guo, N., & Wang, X. P. (2015). Advances and developing opportunities in remote sensing of drought. *Journal of Arid Meteorology, 33*, 1–18.

Hao, C., Zhang, J., & Yao, F. (2015). Combination of multi-sensor remote sensing data for drought monitoring over Southwest China. *International Journal of Applied Earth Observation and Geoinformation, 35*, 270–283. doi:10.1016/j.jag.2014.09.011.

He, J. Y., Zhang, M. J., Wang, P., Wang, S. J., & Wang, X. M. (2011). Climate characteristics of the extreme drought events in Southwest China during recent 50 years. *Acta Geographica Sinca, 66*, 1179–1190.

Jiao, W., Zhang, L., Chang, Q., Fu, D., Cen, Y., & Tong, Q. (2016). Evaluating an enhanced vegetation condition index (VCI) based on VIUPD for drought monitoring in the continental United States. *Remote Sensing, 8*(3), 224. doi:10.3390/rs8030224.

Kogan, F. N. (1995). Droughts of the late 1980s in the United States as derived from NOAA polar-orbiting satellite data. *Bulletin of the American Meteorological Society, 76*, 655–668. doi:10.1175/1520-0477(1995)076<0655:DOTLIT>2.0.CO;2.

Liang, L., Zhao, S., Qin, Z., He, K., Chen, C., Luo, Y., et al. (2014). Drought change trend using MODIS TVDI and its relationship with climate factors in China from 2001 to 2010. *Journal of Integrative Agriculture, 13*(7), 1501–1508. doi:10.1016/S2095-3119(14)60813-3.

Liu, W. T., & Kogan, F. N. (1996). Monitoring regional drought using the vegetation condition index. *International Journal of Remote Sensing, 17*(14), 2761–2782. doi:10.1080/01431169608949106.

Liu, L. W., Zhang, W. P., Duan, Y. H., Xing, L. X., Chen, X. B., & Zhao, M. (2014a). Terrain corrected TVDI for agricultural drought monitoring using MODIS data. *Acta Geographica Sinca, 34*, 3704–3711.

Liu, Z. J., Liu, J. Y., & Shao, Q. Q. (2014b). Optimum temperature of vegetation growth for various land cover types in China. *Journal of Geo-Information Science, 16*, 1–7.

Liu, X., Zhu, X., Pan, Y., Li, S., Liu, Y., & Ma, Y. (2016). Agricultural drought monitoring: progress, challenges, and prospects. *Journal of Geographical Sciences, 26*(6), 750–767. doi:10.1007/s11442-016-1297-9.

Ma, Z., & Fu, C. (2006). Some evidence of drying trend over northern China from 1951 to 2004. *Chinese Science Bulletin, 51*(23), 2913–2925. doi:10.1007/s11434-006-2159-0.

Mao, K., Qin, Z., Shi, J., & Gong, P. (2005). A practical split-window algorithm for retrieving land-surface temperature from MODIS data. *International Journal of Remote Sensing, 26*(15), 3181–3204. doi:10.1080/01431160500044713.

Mao, K. B., Shi, J. C., Li, Z. L., & Tang, H. J. (2007). An RM-NN algorithm for retrieving land surface temperature and emissivity from EOS/MODIS data. *Journal of Geophysical Research: Atmospheres (1984–2012), 112*, 1–17.

Masud, M. B., Khaliq, M. N., & Wheater, H. S. (2015). Analysis of meteorological droughts for the Saskatchewan River Basin using univariate and bivariate approaches. *Journal of Hydrology, 522*, 452–466. doi:10.1016/j.jhydrol.2014.12.058.

Ozelkan, E., Chen, G., & Ustundag, B. B. (2016). Multiscale object-based drought monitoring and comparison in rainfed and irrigated agriculture from Landsat 8 OLI imagery.

International Journal of Applied Earth Observation and Geoinformation, 44, 159–170. doi:10.1016/j.jag.2015.08.003.

Quiring, S. M., & Ganesh, S. (2010). Evaluating the utility of the vegetation condition index (VCI) for monitoring meteorological drought in Texas. Agricultural and Forest Meteorology, 150(3), 330–339. doi:10.1016/j.agrformet.2009.11.015.

Rouse, J. W. J., Haas, R. H., Schell, J. A., & Deering, D. W. (1974). Monitoring vegetation systems in the Great Plains with ERTS. NASA Special Publication, 351, 309.

Sandholt, I., Rasmussen, K., & Andersen, J. (2002). A simple interpretation of the surface temperature/vegetation index space for assessment of surface moisture status. Remote Sensing of Environment, 79(2–3), 213–224. doi:10.1016/S0034-4257(01)00274-7.

Sha, S., Guo, N., Li, Y. H., Ren, Y. L., & Li, Y. P. (2013). Comparison of the vegetation condition index with meteorological drought indices: a case study in Henan province. Journal of Glaciology and Geocryology, 35, 990–998.

Wang, J. S., Li, Y. H., Wang, R. Y., Feng, J. Y., & Zhao, Y. X. (2012a). Preliminary analysis on the demand and review of progress in the field of meteorological drought research. Journal of Arid Meteorology, 30, 497–508.

Wang, Z. M., Yang, H. B., Ji, Q. C., & Li, X. T. (2012b). Remote sensing monitoring for drought in Henan province based on MODIS. Bulletin of Soil and Water Conservation, 32, 139–211.

Wilhite, D. A. (2000). Drought as a natural hazard: concepts and definitions. Drought a Global Assessment, 1, 3–18.

Yan, L. K. (2003). Application of correlation coefficient and biased correlation coefficient in related analysis. Journal of Yunnan University of Finance and Economics, 19, 78–80.

Yin, H., & Li, Y. H. (2013). Summary of advance on drought study in Southwest China. Journal of Arid Meteorology, 31, 182–193.

Zhang, Q., Zhang, L., Cui, X. C., & Zeng, J. (2011a). Progresses and challenges in drought assessment and monitoring. Progresses and Challenges in Drought Assessment and Monitoring, 26, 763–778.

Zhang, Y. D., Zhang, X. H., & Liu, S. R. (2011b). Correlation analysis on normalized difference vegetation index (NDVI) of different vegetations and climatic factors in Southwest China. Chinese Journal of Applied Ecology, 22(2), 323–330.

Zhao, Y. S. (2013). Analysis principle and method of remote sensing application. Beijing: Science Press.

Zhou, D., Zhang, B., Gui, R. P., Zhang, C. L., Yang, S. W., & Ji, D. M. (2014). Analysis of drought characteristics of Shaanxi province in recent 50 years based on standardized precipitation evapotranspiration index. Journal of Natural Resources, 29, 677–688.